Journal of Sound and Vibration (2000) **229**(2), 207–227
Article No. jsvi.1999.2487, available online at http://www.idealibrary.com on IDEAL®

THE ELECTRORHEOLOGICAL LONG-STROKE DAMPER: A NEW MODELLING TECHNIQUE WITH EXPERIMENTAL VALIDATION

N. D. SIMS, D. J. PEEL, R. STANWAY, A. R. JOHNSON AND W. A. BULLOUGH

*Department of Mechanical Engineering, University of Sheffield, Mappin Street, Sheffield S*1 3*JD, England*

(*Received* 28 *January* 1999, *and in final form* 18 *May* 1999)

Semi-active damping devices offer improved performance over passive devices, without the power requirements or instability problems of fully active devices. Smart fluids (electrorheological and magnetorheological) are well suited to use in semi-active dampers—their flow properties can be rapidly altered, with a low-power requirement. However, the force/velocity response is highly non-linear, and this is without doubt hindering the development of effective control strategies. In this paper, the authors develop a new model of an electrorheological damper. The key advantage of this model is that its algebraic form is suitable for use in control system design, whilst it is able to predict and explain observed behaviour. The model consists of a spring, mass, and damper connected in series. The spring stiffness term is based upon the fluid bulk modulus, and the mass is determined from the fluid density. The damping characteristic utilizes a modified non-dimensional Bingham Plastic function. The model predictions are compared with experimental results at a range of operating frequencies. Excellent agreement was achieved by updating the stiffness and viscosity parameters using experimental data.

1. INTRODUCTION

Vibration isolation is a field of engineering that has seen great developments in recent years. In part, this has been made possible by the development of high-speed, affordable computers—both from a design and development perspective, and for use in real-time control. However, the driving forces have often come from the market place. In road and rail vehicle suspensions there is a tangible gain in improving passenger comfort and safety in all areas of the market, from Formula One racing cars and high-speed trains to military vehicles [1]. The same can be said for structural applications, where there is a need for improved comfort in wind-excited tall buildings, and seismic protection is essential in some parts of the world [2].

At the forefront of these developing technologies are the so-called "semi-active" devices [3]. Like active devices, these are able to adapt readily to suit their changing environment, albeit in a longer time scale. However, unlike active devices,

0022-460X/00/020207 + 21 $35.00/0

they do not directly increase the energy of the vibrating structure. This makes them more intrinsically stable, as well as having a lower power requirement.

Electrorheological devices (and their Magnetorheological counterparts) are well placed in the semi-active niche. They are able to react quickly to duty requirements, and yet have a relatively low-power requirement—typically less than 20 W. Whilst the cost of prototype devices and fluids is still high, more affordable production devices are starting to appear [4].

An ER fluid consists of solid particles suspended in a carrier liquid. When an electric field is applied, the particles are polarized and form chains between the electrodes. This chain structure is held in place by the field, and hence resists fluid flow. The resulting behaviour is analogous to the class of fluids known as Bingham Plastics—non-Newtonian fluids capable of developing a yield stress which is a function of the applied electric field. Once the "yield stress" is exceeded, however, the behaviour of the fluid deviates from that of an ideal Bingham Plastic. This is attributable to the breakdown of the chains of particles under the forces of the fluid flow. Magnetorheological devices harness the same phenomena but use magnetic fluids and fields rather than ER fluids and electric fields. Similar modelling techniques have been applied to both devices [4].

There are three main configurations for ER dashpot damper devices: flow, shear, and squeeze. In flow mode, the fluid is forced between a pair of stationary electrodes, and the resistance to flow is controlled by adjusting the applied electric field. This "flow control valve" bypasses the piston in the damper, and is the form of the device used in this study. In shear mode, the electrodes are able to translate in relation to each other. This occurs if they are placed on the piston and cylinder walls, and the fluid is forced between them. Finally, in squeeze mode, the fluid between the electrodes is squeezed as the electrode gap changes. This occurs when the electrodes are placed on the piston head and cylinder end.

It is apparent from the above that ER damping devices can be made in a variety of configurations. A whole host of design attributes can be adjusted: stroke length, maximum force, minimum damping level, to name but a few. This has resulted in a diverse range of academic and industrial prototypes and some production models [5]. The specific merits of each, along with the merits of ER fluid versus MR fluid, is a subject in itself. However, they all posses one attribute: their response is significantly non-linear.

This non-linearity has undoubtedly hindered the development of industrial applications. There are two reasons for this: first, it is difficult for us to understand the fluid's behaviour, and second, it is difficult to control the fluid's response.

In this paper, our aim is to develop a new model of an ER damper, capable of predicting and *explaining* the observed response. Firstly, the ER damper test rig, on which the model is based, is introduced. Then, a number of existing models are described. This illustrates the need for our new modelling perspective. The new model is then developed, and the simulations compared with experimental results.

2. ER DAMPER TEST RIG

The test rig is essentially an ER long-stroke damper, driven by a sinusoidal displacement input from a variable speed motor. In this section, the rig is described

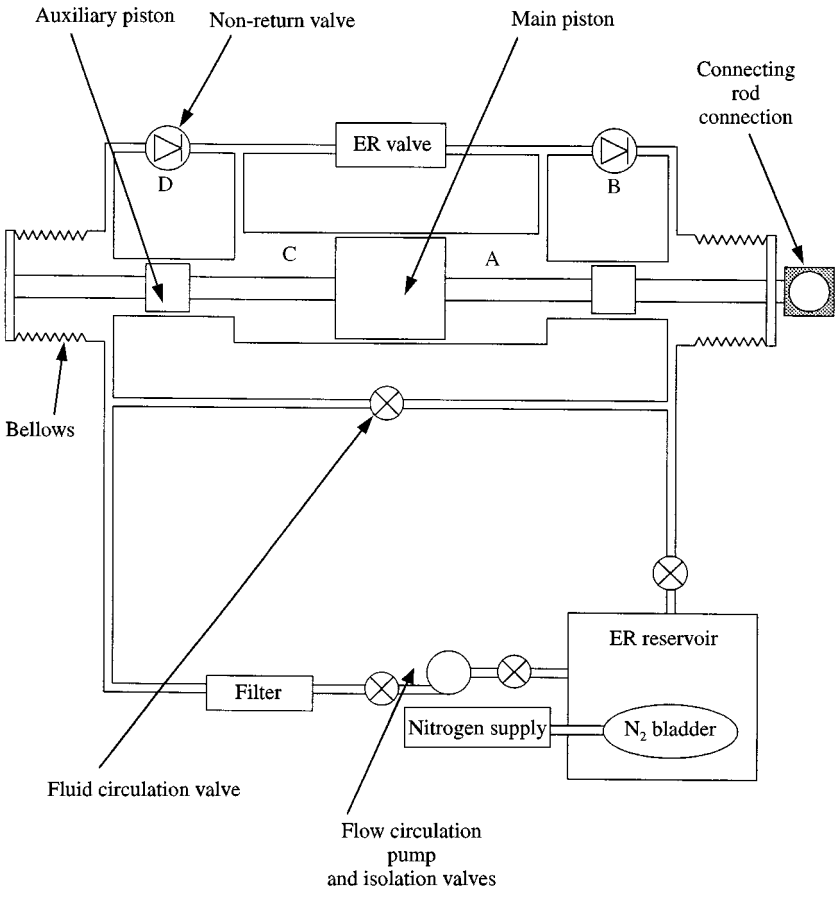

Figure 1. Damper test rig—ER fluid system.

in detail, in terms of the ER fluid system, the cooling water system, the driving system, and the instrumentation.

The fluid system consists of the damper cylinder, pistons and valves, and a nitrogen pressurized accumulator. Fluid homogeneity is ensured by a circulation pump and filter. The operation of the device can be explained with reference to Figure 1. As the piston moves from left to right, the volume A decreases, and the non-return valve B remains shut, forcing fluid through the ER valve. Meanwhile, the volume C increases, and the non-return valve D opens, relieving this side of the main piston to the bladder pressure. The fluid circulation valve, being open, ensures that fluid is not drawn through the pump and filter during operation of the device. The auxiliary pistons ensure that the pressures at the ends of the cylinder are always the same as the bladder pressure, thus enabling the use of bellows, which avoids the problems associated with sealing the slurry-like liquid. The design also reduces the problems of cavitation of the fluid on the low-pressure side of the piston, since the pressure in this region is maintained at the bladder pressure. The ER valve consists

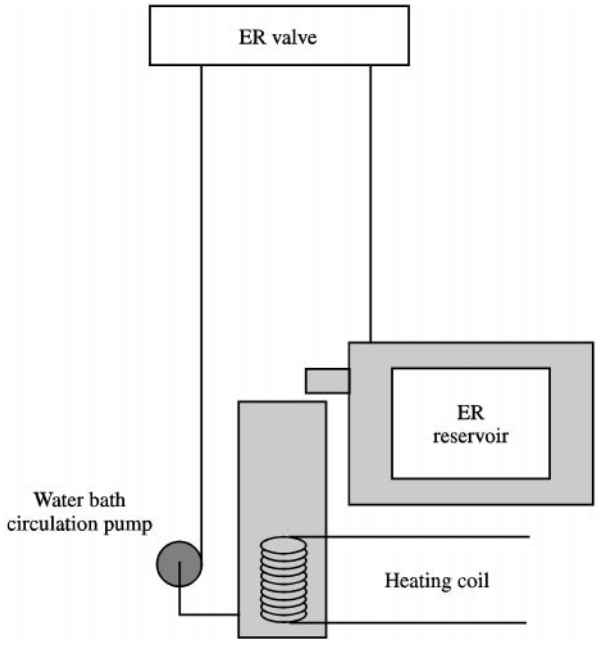

Figure 2. Damper test rig—cooling water system.

of annular concentric electrodes of opposing electric polarity. Application of this electric field results in an increased resistance to flow across the piston head, and hence a pressure drop across the valve. The force on the main piston is therefore given by this differential pressure times the effective piston area.

The fluid is cooled using a water bath arrangement as shown in Figure 2. The water circulation pump maintains a flow of water around the ER valve cooling shell, the accumulator water bath, and the heating coils. The water temperature can be controlled using the heating coils.

The piston is driven using a variable-speed electric motor, via a reduction gearbox and cam arrangement. The gearbox has four reduction settings, offering an output shaft speed between 150 and 1500 r.p.m. for an input speed of 1500 r.p.m. This enables the piston frequency to be chosen as any value up to 25 Hz. Piston stroke is adjustable off-line by moving the connecting rod along the crank arm. The maximum piston displacement is 16 mm, limited by the cylinder length.

Finally, data are collected on a PC via a data logger, allowing sampling frequencies in the region of 1 kHz. The main measurement variables are as follows: cylinder chamber pressure on each side of the main piston, cooling water temperature in the valve and baths, piston displacement and trigger signal, and ER valve voltage level. The valve voltage is selected using a high-voltage generator with remote input, allowing an applied electric field strength of up to 8 kV/mm.

3. DAMPER MODELS

There have been many attempts to model the behaviour of ER and MR dampers [4]. This modelling has three main objectives: firstly, it can be used as a design tool for the sizing of prototype devices. Secondly, it deepens our understanding of ER/MR fluid behaviour, and thirdly, it helps us to design suitable control systems.

Static ER models were available in the 1980s, but were of limited usefulness. It is now apparent that dynamic effects, such as compressibility and inertia, exert a significant influence upon a damper's response [4]. This is particularly the case in the region of fluid flow reversal, where hysteretic behaviour can be seen in the force–velocity characteristic. An example of an early model is the one developed by Stanway *et al.* [6]. This model combined dry friction and viscous elements to produce a response analogous to an ideal Bingham Plastic. This model was the precursor to many of the more recent "phenomenological" type models. These are models that have combined viscous, Coulomb, stiffness, and inertia elements to form a suitable lumped parameter system. This has enabled the inclusion of dynamic effects, such as fluid compressibility and inertia. However, the resulting models are often complex and difficult to solve. Examples are the model proposed by Gamota and Filisko [7], having three degrees of freedom, and the extended Bouc-Wen model proposed by Spencer *et al.* [3], which was able to model hysteresis, but did little to explain it.

Other approaches have also been taken in recent years, such as neural networks [8], and Chebyshev polynomial techniques [9]. Whilst the models can agree well with experimental data, they generally fail to explain the observed behaviour.

At the University of Sheffield, work has concentrated on obtaining a deeper understanding of the quasi-steady response. Peel *et al.* [10] developed a non-dimensional technique to characterize ER fluid behaviour, and this has been extended in recent years to include dynamic effects. In the following sections, the authors derive a mass–spring–damper model incorporating the non-dimensional characterization developed previously [10]. This results in a model that accounts for, and *explains* the observed dynamic behaviour in a working ER long-stroke damper test rig. Furthermore, the model is in a form that is suitable for control system design.

4. OVERVIEW OF THE NON-DIMENSIONAL CHARACTERIZATION

Before developing a lumped parameter model that is capable of explaining dynamic effects, it is necessary to have an understanding of the non-demensional methodology that will be used to define the damper's quasi-steady response. The non-demensional method is based upon the well-known Bingham Plastic constitutive equation for flow through two parallel plates [11]:

$$4\left(\frac{l}{h\Delta P}\right)^3 \tau_b^3 - 3\left(\frac{l}{h\Delta P}\right)\tau_b + \left(1 - \frac{12\mu l Q}{bh^3 \Delta P}\right) = 0, \tag{1}$$

where l is the valve (i.e., plate) length, h is the electrode (i.e., plate) gap, b is the electrode circumference (i.e., plate width), ΔP is the pressure drop across the valve, τ_b is the fluid yield stress, μ is the fluid viscosity, and Q is the volume flow rate. Of the three roots to this cubic equation, two are inadmissible: one of the roots gives a negative value for ΔP, and the other requires a shear stress at the channel wall less than the Bingham yield stress. Since the shear stress will be greatest at the channel wall, this is inadmissible if flow is to occur. The remaining physically meaningful root is the one with the largest positive value, and can be used to evaluate the pressure drop across the channel.

Peel and Bullough [12] showed that equation (1) can be rewritten in terms of the following dimensionless groups:

$$\pi_1 = \frac{\Delta P h}{2 l \rho \bar{u}^2} \quad \text{(friction coefficient)},$$

$$\pi_2 = \frac{\rho \bar{u} h}{\mu} \quad \text{(Reynolds number)},$$

$$\pi_3 = \frac{\tau_b \rho h^2}{\mu^2} \quad \text{(Hedström number)}, \tag{2}$$

where ρ is the fluid density and $\bar{u}$ is the mean fluid velocity, Q/bh. Substituting these terms into equation (1) gives

$$\pi_1^3 - \left(\frac{3}{2} + 6\frac{\pi_3}{\pi_2}\right)\left(\frac{\pi_3}{\pi_2^2}\right)\pi_1^2 + \frac{1}{2}\left(\frac{\pi_3}{\pi_2^2}\right)^3 = 0. \tag{3}$$

The Bingham yield stress has been measured by Peel and Bullough [12], using an ER clutch mechanism, resulting in an empirical relationship between field strength and yield stress. Other parameters are readily determined from the fluid's properties and valve dimensions.

The key to the dimensionless approach is that it enables the use of empirical coefficients to correct for observed flow behaviour. Whilst an ideal Bingham Plastic exhibits a yield stress that remains constant during flow, the ER fluid changes its properties as flow starts. This can be explained by a breakdown in the chains of semi-conducting particles, resulting in a decrease in the resistance to flow. This can be accounted for by defining a "dynamic" Hedström number, which is a function of the static Hedström number, and Reynolds number [12].

In the case of our damper, equation (3) applies to the flow in the ER valve, assuming that the concentric design of the device can be approximated to flow between parallel flat plates. The pressure drop across the valve gives rise to a corresponding force F on the piston, defined by introducing the modified Bingham Plastic function

$$F = \chi(u, E, h, l, \rho, \mu, A), \tag{4}$$

where u is the piston velocity (from which the flow rate in the valve Q can be determined), E is the electric field across the valve, and A is the area of the piston.

The force is due the differential pressure ΔP, obtained from the admissible root of equation (3) acting over an area A. For a more detailed description of this methodology, the interested reader is referred to reference [12].

5. DERIVATION OF A SPRING–MASS–DAMPER MODEL

By considering the physical arrangement of the long-stroke damper, and making some intuitive simplifications, one can develop a simple model of the damper's behaviour. As a first step, consider the layout of the damper as described in section 2. A simplified representation of the device is shown schematically in Figure 3. Whilst the quasi-steady ER effects that occur in the valve can be incorporated into the modified Bingham Plastic damper function described above, it is the fluid's compressibility and inertia that are the main contributors toward dynamic effects. In a lumped parameter model, the fluid's compressibility can be expressed as two springs of stiffness k, one running from each side of the piston to the ER valve, whilst the fluid's inertia can be represented by a lumped mass m at the piston head. If we now think of the model as being "unwound" at the valve (or damper), then the system shown in Figure 4 is obtained.

The drawback with this simple representation is that it does not account for the physical arrangement of the piston mechanism, as described in section 2. This arrangement has overcome the problems associated with the use of particle suspensions in hydraulic systems, such as sealing the unit at the shaft/cylinder

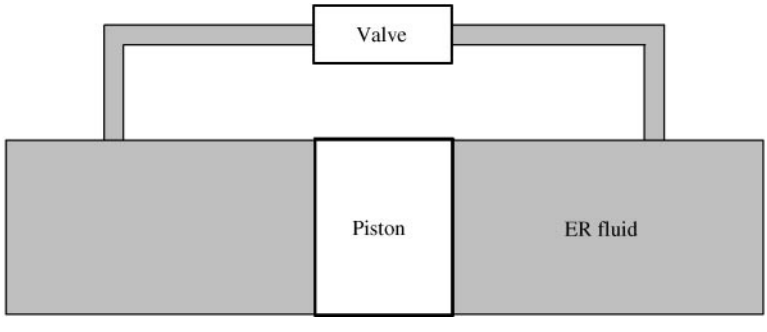

Figure 3. Piston and cylinder schematic.

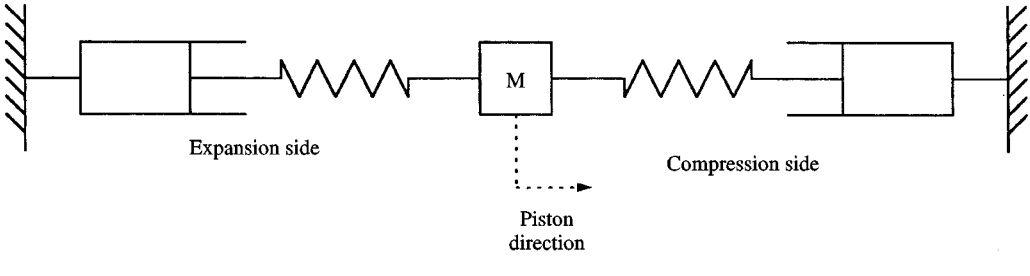

Figure 4. Lumped parameter representation.

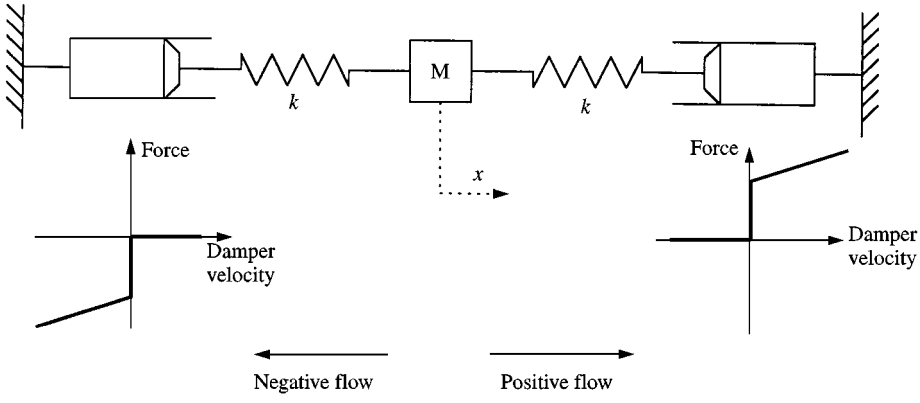

Figure 5. Adapted lumped parameter model.

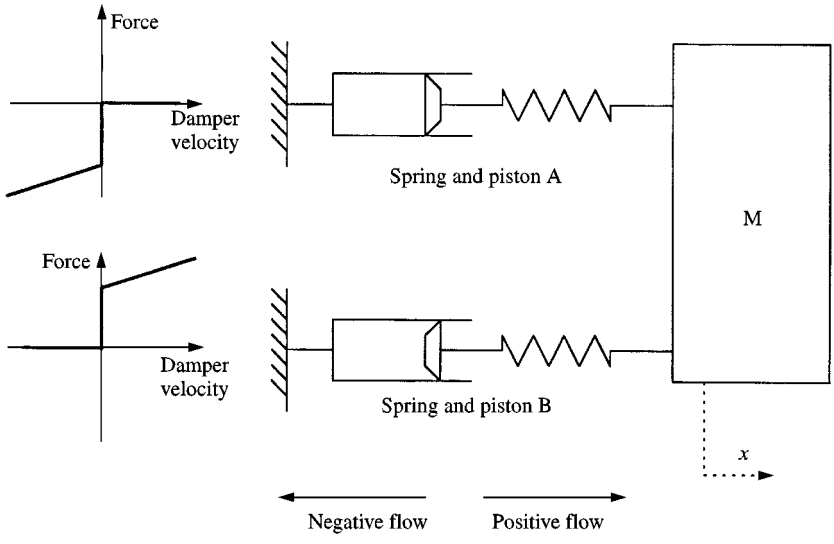

Figure 6. Lumped parameter model, rearranged.

interface. The resulting design is such that the compression side of the piston (as defined in Figure 4) is "relieved" to the bladder pressure (0·7 bar g). This aspect of the response can be built into the model by specifying dampers that do not resist expansion flow. The resulting model is shown in Figure 5. This model, however, can be rearranged to reduce the number of parameters. Consider a corresponding model, shown in Figure 6. This will give the same response, but has both dampers on the same side of the mass. It is apparent that this model has three distinct operating regions:

- When damper velocity is positive, damper B is resisting motion, whilst damper A and spring A are transmitting no forces.

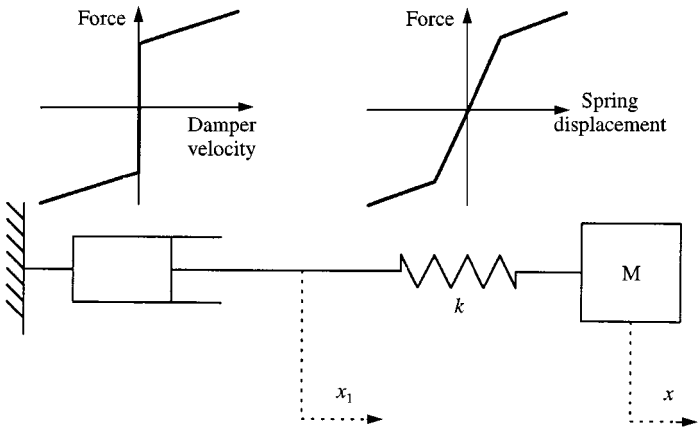

Figure 7. Simplified lumped parameter model.

- When damper flow comes to a stop, both dampers become rigid, and both springs resist motion.
- Once flow has reversed, damper A resists motion, whilst damper B and spring B are transmitting no forces.

From these observations, it is logical to combine the two springs to form one bilinear spring, and to combine the dampers in similar fashion. The resulting model is shown in Figure 7. The equations of motion for this system are

$$-\chi(\dot{x}_1, E, h, l, \rho, \mu, A) + \kappa(x - x_1) = 0,$$
$$F - \kappa(x - x_1) = m\ddot{x}, \tag{5}$$

where x is the applied motion, x_1 is the displacement of the damper, and F is the corresponding piston force. χ is the modified Bingham Plastic function, as defined in the previous section, and κ is the bilinear spring function:

$$\kappa(x) = \begin{cases} 2kx & \text{if } |x| \leqslant \dfrac{F_y}{2k}, \\ kx - F_y/2 & \text{if } x < -\dfrac{F_y}{2k}, \\ kx + F_y/2 & \text{if } x > \dfrac{F_y}{2k}, \end{cases} \tag{6}$$

where F_y is the yield force resulting from the applied electric field.

Hence, the final form of the lumped parameter model has been developed. However, before going on to develop a numerical technique for solving the model, we must estimate values for the parameters k and m. Tentative values are obtained by calculating the mass directly from the volume of working fluid and its density. The stiffness is calculated in a similar fashion, using the fluid's bulk modulus. The accuracy of the values thus determined, and ways of obtaining improved estimates, are discussed later.

6. NUMERICAL METHODS

In this section, possible methods of solving the equations of motion for the lumped parameter system are investigated. Two problems arise in the solution of equation (4) firstly, the damper function involves a step discontinuity at flow reversal, which poses numerical problems. Secondly, the absence of an inertia term between the spring and damper makes it impossible to express the equations in state-space form in a straightforward fashion. We present two methods of overcoming these problems.

In the first technique, the discontinuity is overcome using a suitable logic system in the numerical calculations. This technique has been used for similar numerical problems, such as stick-slip friction [13]. The logic system detects the onset of flow reversal in the valve, and effectively locks the damper in its current position. The damper is "unlocked" from this position when the spring force pushing against the damper exceeds the yield force for the fluid. Although the equations cannot be expressed in conventional state-space form, modern simulation software [14] can be employed to solve the equations in an alternative fashion. The equations of motion (4) are expressed in a block diagram form, as shown in Figure 8. It can be seen that equation (4) is a non-linear algebraic equation which must be solved iteratively. In the block diagram notation [14], this is represented by an algebraic

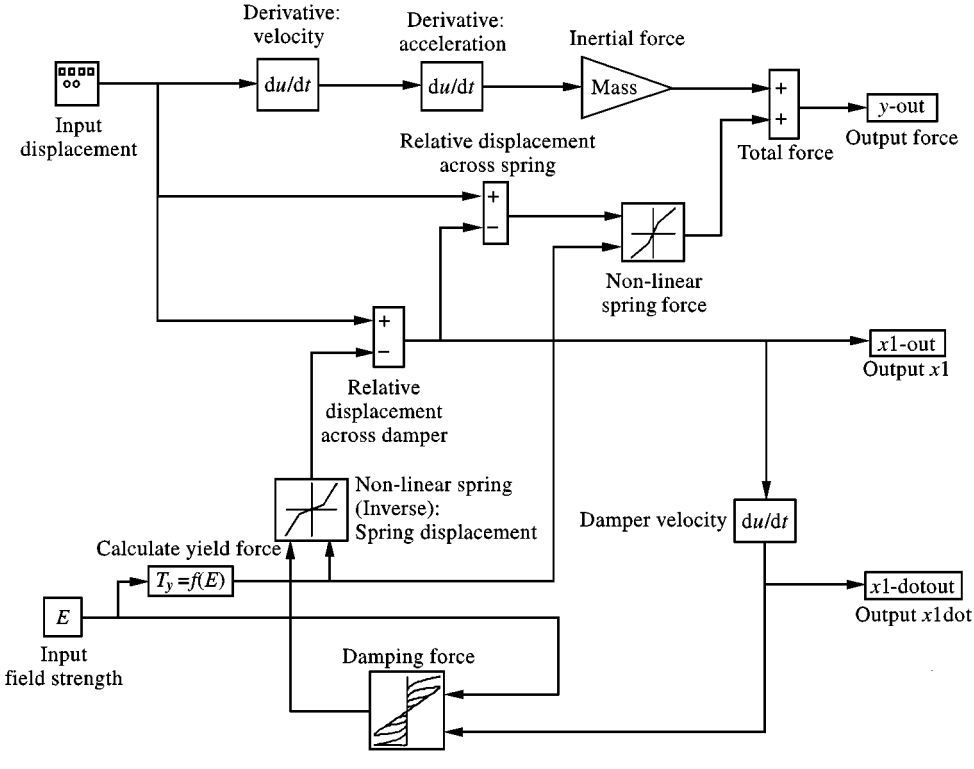

Figure 8. Block diagram representation of equation (5).

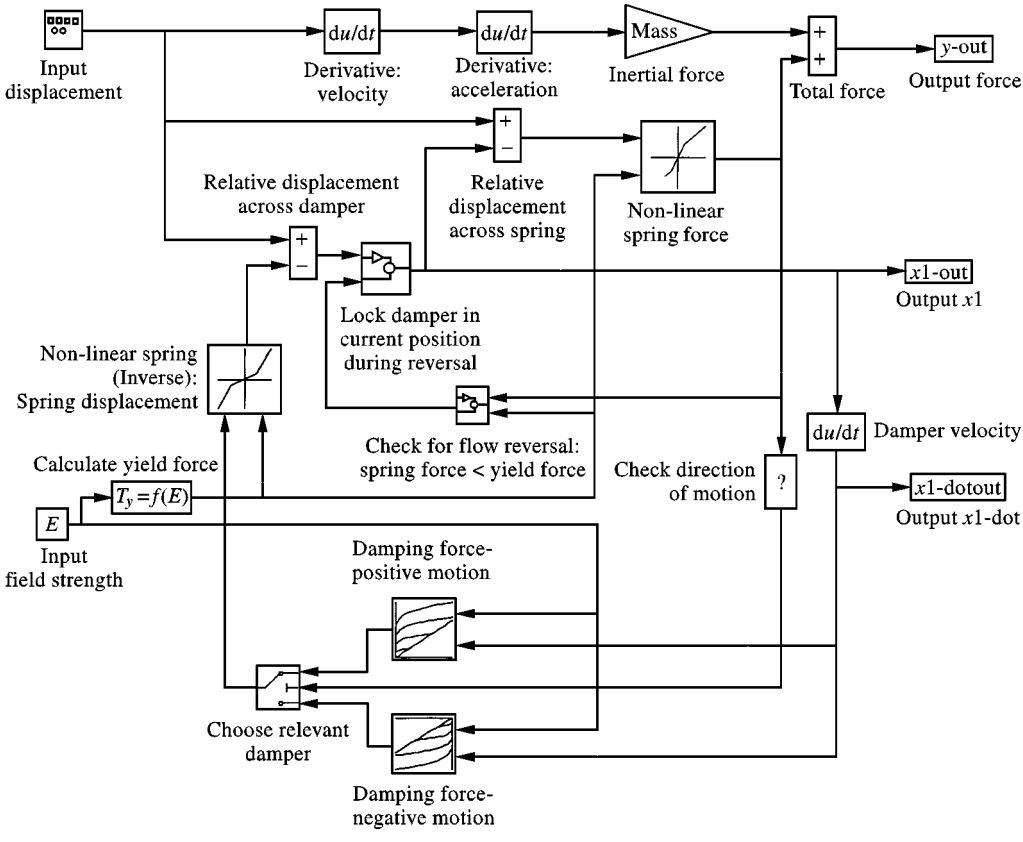

Figure 9. Modified block diagram to include two lookup tables and a logic system.

loop, i.e., a set of blocks where "direct feedthrough" forms a feedback loop. Direct feedthrough occurs when the output of a block at any time is a function of the input at that time. The algebraic loop must be solved iteratively using the Newton–Raphson technique. However, it is apparent that the algebraic loop contains the discontinuous damping function. This poses a problem, since Newton's method involves computing the first derivative of the function, which is undefined at the step discontinuity. One solution to this problem is to define two separate dampers, using a lookup/extrapolation function. Switching between the two dampers occurs at flow reversal, when the damper is locked in position by the logic system. At other times, the software linearly interpolates between the data values in the lookup table for the appropriate damper. Since extrapolation is used for iteration points that lie outside the damper's defined region, the software no longer senses the discontinuity. The block diagram incorporating this modification is shown in Figure 9.

The second technique involves a more elegant approach to the problem. As a first step, the equations of motion are rewritten in the following form:

$$\dot{x}_1 = \chi^{-1}(\kappa(x_2 - x_1, E), E, h, l, \rho, \mu, A),$$
$$F = \kappa(x_2 - x_1, E) + m\ddot{x}_2, \tag{7}$$

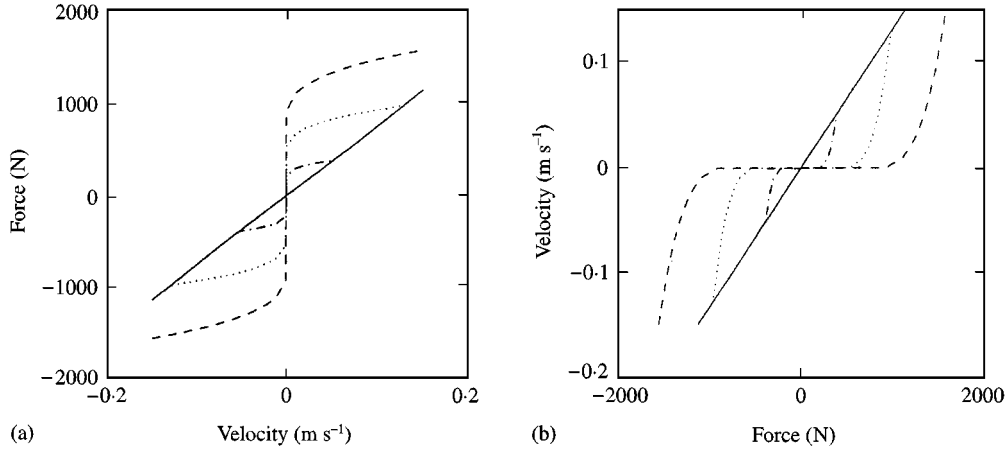

Figure 10. Inverse damper function: (a) force/velocity characteristic showing infinite gradient at flow reversal; (b) velocity/force characteristic showing zero gradient at flow reversal. ——, 0 kV/mm; - - - - - - - - -, 1 kV/mm; ·····, 2 kV/mm; ---------, 3 kV/mm.

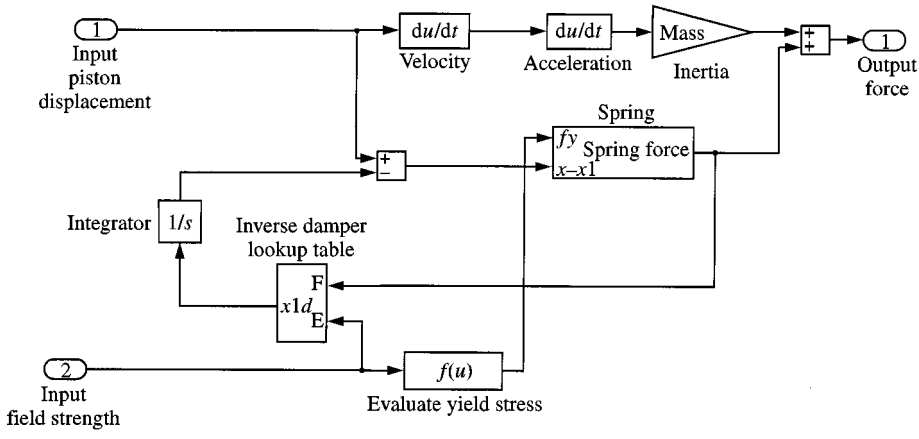

Figure 11. Block diagram incorporating the inverse damper function.

where χ^{-1} is the inverse modified Bingham Plastic damper function, which calculates the velocity across the damper for a given force.

Now, the non-linear algebraic equation has been replaced by a first order ordinary differential equation, involving the inverse damper function χ^{-1}. This not only does away with the algebraic loop, but also alleviates the problem of the discontinuity at flow reversal, since the discontinuity now has zero gradient, rather than infinite gradient. This is shown in Figure 10, and a block diagram for this second approach is shown in Figure 11.

All that remains is to develop a numerical method to evaluate the inverse damper function χ^{-1}. Recall that the damper force is a function of field strength and velocity. The inverse function requires the value of the damper velocity at a given

field strength and force. One method is to solve the inverse function iteratively, using the bisection method for example. However, a more convenient technique is to generate a lookup table. This allows the simulation to run much faster, since the computations required during simulation are greatly simplified. The lookup table is easily generated. First, a set of solutions to the damper function is created, for a given field strength. These data are then used to interpolate a set of velocity values at equally spaced forces, and the routine is repeated for a set of equally spaced field strengths. Provided a sufficient number of original data points are taken, the error between the linearly interpolated value of the inverse function, and its actual value, will be negligible.

The second method, involving the inverse damper function, was chosen as the preferred technique for the simulations.

7. EXPERIMENTAL AND MODEL RESULTS

Having developed a model of the ER damper and shown how to solve it, the model's results are compared with the experimental data. The response at 1, 2, and 3 Hz, will be investigated using a range of electric fields. The displacement amplitude is held constant at $\pm$ 8 mm.

Firstly, consider the response at 1 Hz, with zero field strength, as shown in Figure 12. It can be seen that the damper's response is linear, like a simple dashpot damper. This is to be expected in the zero electric field condition, since the ER fluid should behave as a Newtonian fluid, with no developed yield stress. It is immediately apparent, however, that the damping coefficient predicted by the model (i.e., the slope of the force/velocity characteristic) is almost double than that measured experimentally. This highlights one of the characteristics of ER fluid: significant variations in viscosity. As with any oil, the viscosity is highly dependent on the

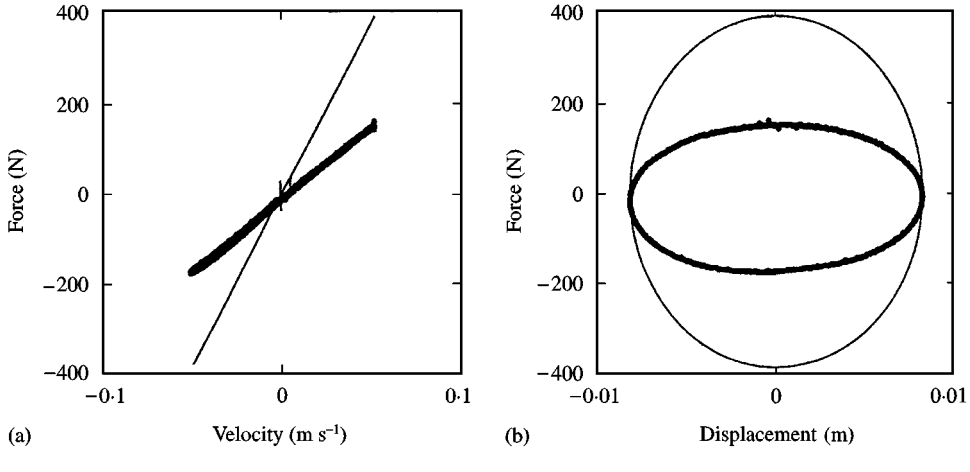

Figure 12. Response at 1 Hz, 0 kV/mm. (a) force/velocity; (b) force/displacement. ●●●, Experimental; ———, predicted.

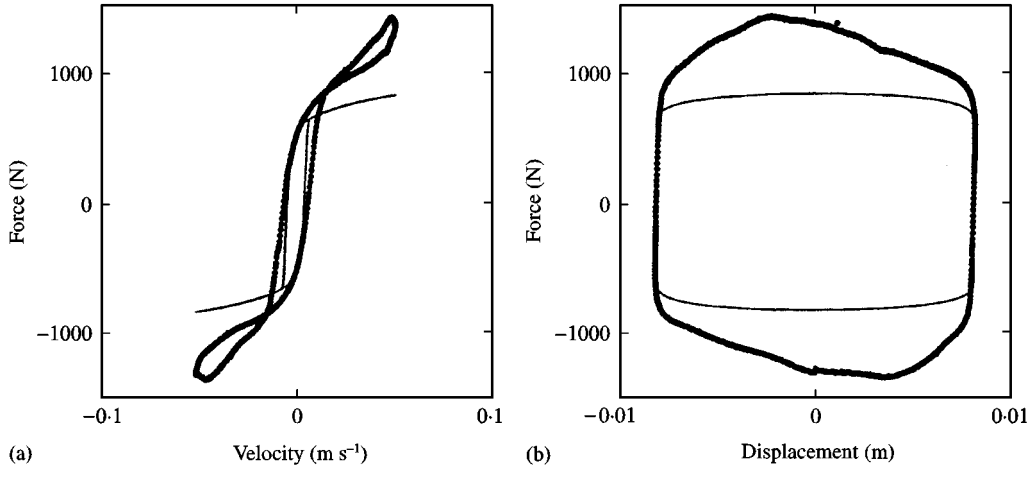

Figure 13. Response at 1 Hz, 2 kV/mm. (a) force/velocity; (b) force/displacement. ●●●, Experimental; ———, predicted.

temperature, but it is also thought to be influenced by variations in the volume fraction of the solid particles suspended in the fluid. Changes in volume fraction occur slowly (i.e., over a period of several days) as the fluid is circulated and allowed to rest. The viscosity value used in the model was based upon manufacture's data, and so the batch of fluid in the test rig may exhibit different properties. Another observation from Figure 12 is that the effects of fluid compressibility, manifested as hysteresis in the force/velocity response, are negligible. The zero electric field response at higher frequencies (2 and 3 Hz) was similar, with similar magnitudes of error in the assumed value of model viscosity.

The response under an electric field of 2 kV/mm is now investigated. Figure 13 shows the experimental and predicted response at 1 Hz. The electric field has created a yield stress in the fluid, equivalent to a 800 N force. Below this yield stress, the flow through the ER valve is arrested, and the fluid's compressibility has introduced a hysteresis loop into the force–velocity relationship. The model has adopted a similar shape of response to the experimental results, with good prediction of the hysteresis at flow reversal. However, the yield force appears to be higher than predicted. Again, this can be explained by variations in the volume fraction of the fluid through time, and by differences in the batches of fluid. We can also see that the slope of the experimental response at higher velocities is considerably greater than that predicted by the model, with a significant "loop" present in this region. With reference to Figure 14, one can see that the slope of the response decreases at higher frequencies. This is probably due to a higher flow velocity being achieved in the valve. The hysteresis loop at flow reversal increases in size with frequency. The 2 Hz response is shown with its model prediction in Figure 15, and one can see that there is better agreement between the two. There are two discrepancies: first, the differences in yield point discussed previously, and second, a variation in fluid compressibility. This variation can be seen as a smaller

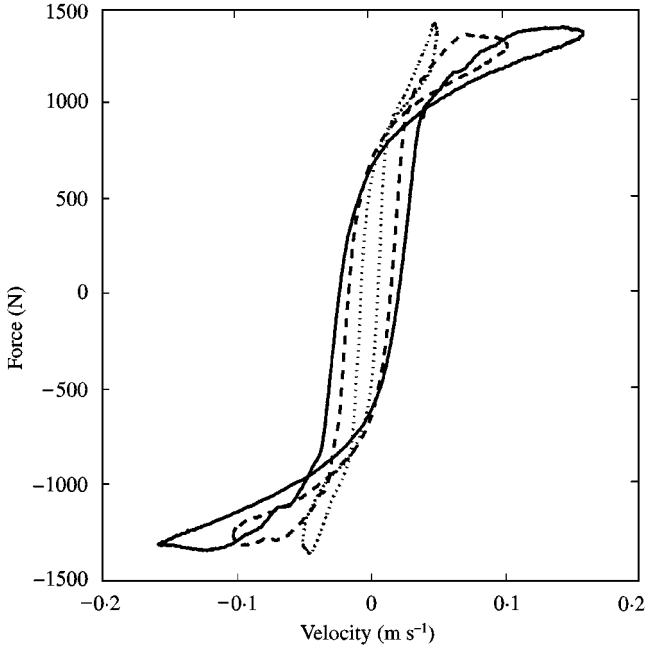

Figure 14. Experimental response at 1, 2, 3 Hz. 2 kV/mm field strength. ⋯⋯, 1 Hz; ------, 2 Hz; ———, 3 Hz.

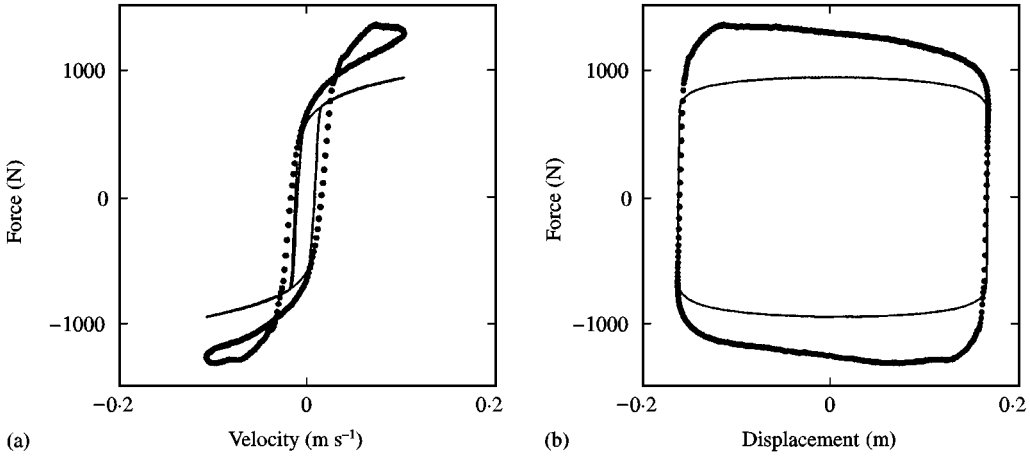

Figure 15. Response at 2 Hz, 2 kV/mm: (a) force/velocity; (b) force/displacement. ●●●, Experimental; ———, predicted.

hysteresis loop in the force–velocity plot, and a steeper slope at flow reversal in the force–displacement plot. According to our model, the damper's stiffness during flow reversal should be a function of the fluid compressibility. One can therefore

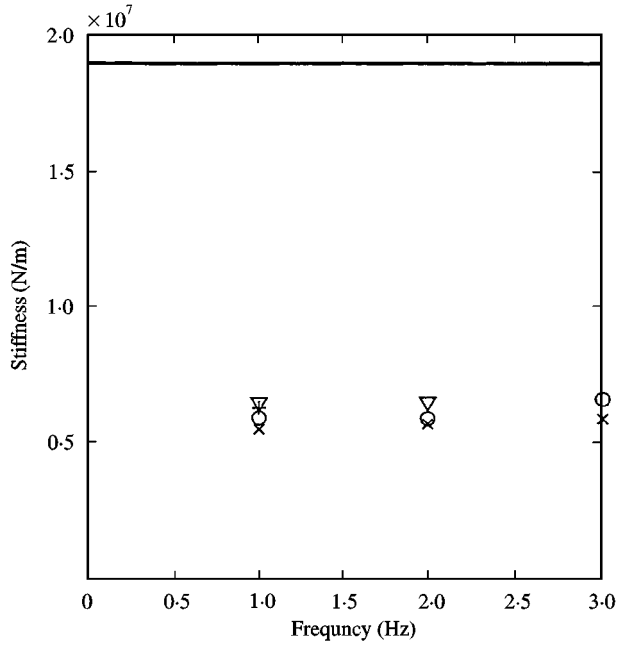

Figure 16. Experimental stiffness and model stiffness. ○○○, 1 kV/mm; ▽▽▽, 2 kV/mm; × × ×, 3 kV/mm; + + +, 5 kV/mm; ———, predicted value.

measure the slope of the experimental force–displacement response in this region, and compare it with the stiffness term used in the model. This is shown graphically in Figure 16. There is a slight variation in experimental stiffness with both field strength and frequency, but the model stiffness is between three and four times the actual measured value. The model stiffness was calculated using bulk modulus values specified by the manufacturer, and again there will be some variation in the actual value between batches. Variations in volume fraction may also affect the stiffness, and there may also be entrapped air in the system, thus reducing its stiffness.

The responses at 3 Hz are shown in Figure 17. The same discrepancies are present: a difference in yield stress, fluid stiffness, and fluid viscosity. However, the values of the corresponding model parameters can be updated using the observed experimental behaviour. The stiffness can be adjusted using the data shown in Figure 16. The viscosity can be updated using a similar technique: fitting a straight line to the zero electric field response, and using its slope to calculate the fluid viscosity. The field strength is less easy to update, but can be adjusted to minimize the difference between experimental results and model predictions. Using the revised parameter estimates, the model prediction is greatly improved, as shown in Figure 18.

As the above experiments involve steady state responses to sinusoidal excitation, it is also instructive to investigate the response of the ER damper to a step change in field strength. As a worst case, consider an excitation frequency of 4 Hz, and

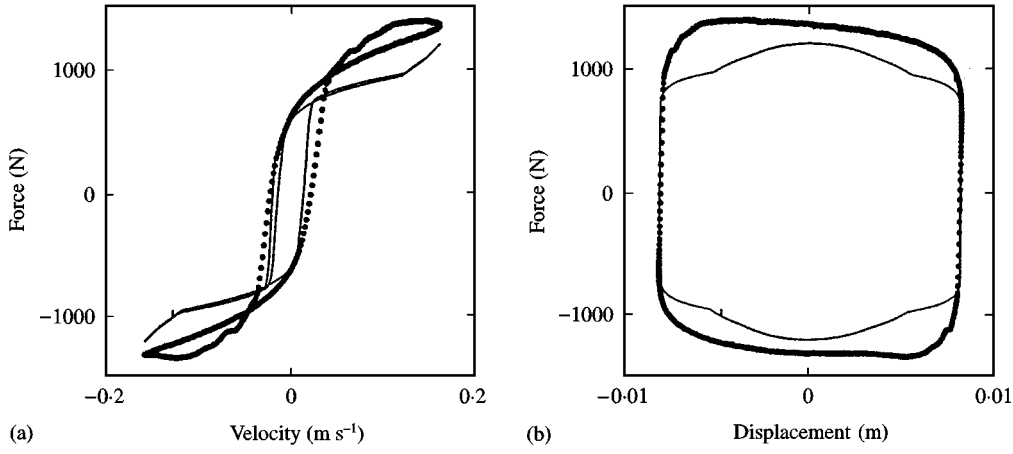

Figure 17. Response at 3 Hz, 2 kV/mm: (a) force/velocity, (b) force/displacement. ●●●, Experimental; ———, predicted.

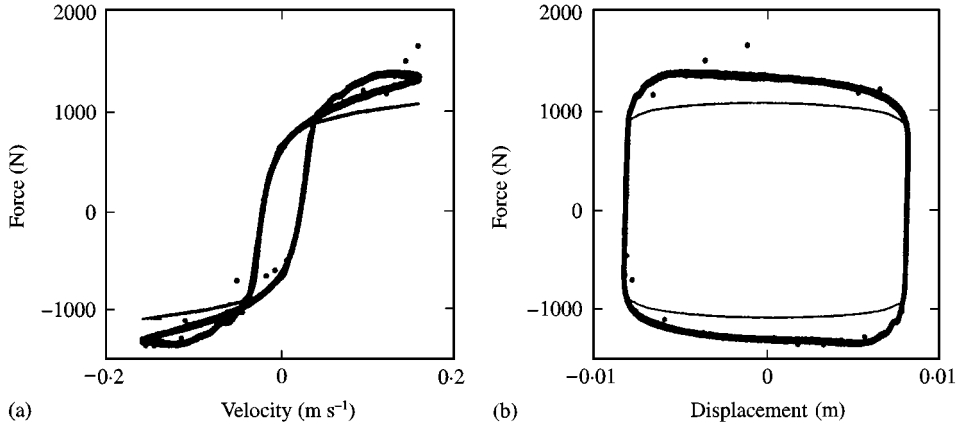

Figure 18. Response at 3 Hz, 2 kV/mm, adjusted parameter values: (a) force/velocity; (b) force/displacement. ●●●, Experimental; ———, predicted.

a electricfield step change from 0 to 4 kV/mm. The model parameters (stiffness, yield point, and viscosity) were updated to give good agreement at constant voltage. The response is shown in Figure 19. The force–time plot shows four cycles of the piston, with the voltage being stepped on and off on each cycle. The first cycle is at 4 kV/mm, and the voltage is switched off at about 1 s. One cycle later, at about 1·2 s, the voltage is again switched on. We can see that the predicted response shows excellent agreement with the experimental response. Figure 20 zooms in on the voltage step at about 1·2 s. It can be seen that the system reacts almost instantaneously, and that the model tracks this response accurately. Overshoots occur in the experimental response which are not observed in the prediction. These are probably caused by the fluid inertia, and the model is unable to predict this since the fluid inertia is constrained at the piston head. A more complex model,

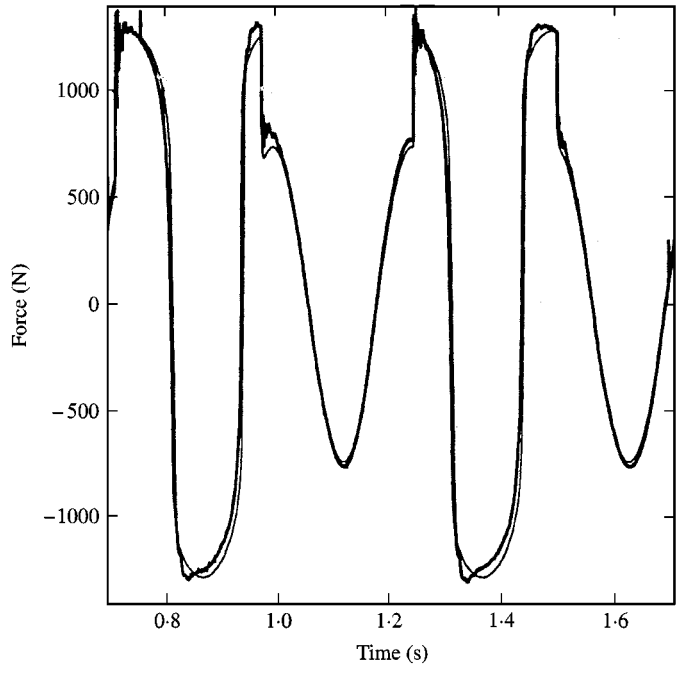

Figure 19. Response to a step change in field strength, 0–4 kV/mm. ———, Experimental; – – – –, predicted, adjusted parameters.

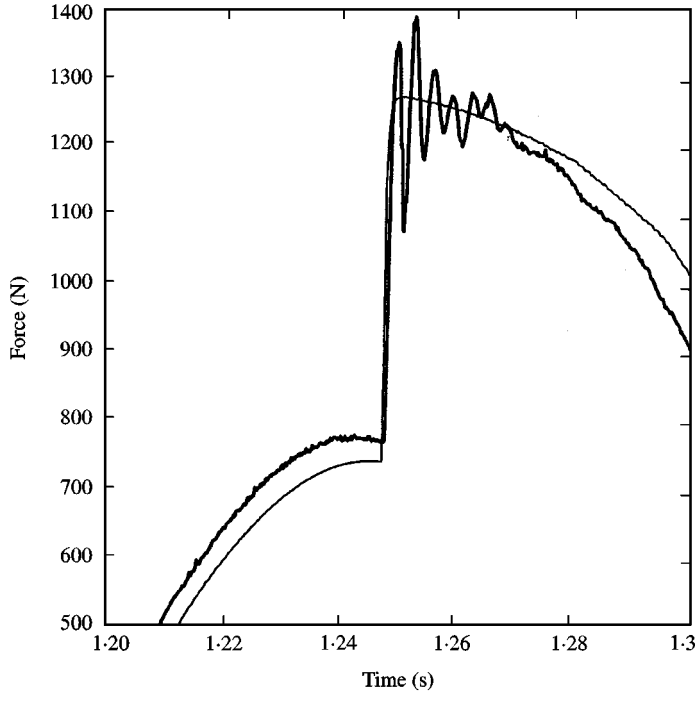

Figure 20. Response to a step change in field strength, 0–4 kV/mm. 4 Hz (zoomed in).

involving additional degrees of freedom, would emulate this distributed system response more accurately, but at the expense of additional computation time.

8. DISCUSSION

A form of model has been developed which is capable of predicting the response of the ER long-stroke damper at various operating conditions. It has been shown that there are significant errors in the model's predictions, but that these originate mainly from the parameters values in the model, rather than in the model structure. Such model parameters are sensitive to various environmental factors: temperature, fluid volume fraction, entrapped air in the fluid, differences between fluid batches, etc., and initial values were chosen using manufacturer's data and fundamental engineering principles, rather than making use of observed behaviour. By making revised estimates of some the parameters, good agreement was achieved between experimental and predicted results. The model accurately predicted the response to step changes in voltage, indicating that it is in a form suitable for the investigation of control strategies.

Investigation of the damper's response at higher frequencies is required, where it is expected that the effects of fluid compressibility and inertia will be greater. It is expected that the "overshoots" observed in Figure 20 will increase in size at higher frequencies, causing discrepancies between model predictions and experimental results. The influence of displacement amplitude on the response is also yet to be investigated.

It is also apparent from the results presented that further work should concentrate on accurately identifying the model parameters to improve the accuracy of the predictions. However, it should be noted that the observed values of these parameters can change on a day-to-day basis, due to fluctuations in the environment. This means that it is important to develop a control strategy for the damper that is robust in the face of model variations [15]. Such a strategy could be developed using the existing model, and then tested by varying the damper model parameters and investigating changes in the response.

9. CONCLUSIONS

A model of an ER long-stroke damper has been developed which is capable of predicting and explaining the observed behaviour in a working test rig. The model is based on our knowledge of ER fluid in quasi-steady flow, and is extended for the dynamic case by incorporating fluid compressibility and inertia. The model can be expressed in a form which is readily solved using standard software, and which can be used for the simulation of control strategies. Model predictions have been compared with experimental results at operating frequencies below 5 Hz, and over a range of electric field strengths. The shape of the model predictions compared well with the shape of the observed response, particularly in the region of flow reversal. The accuracy of the original model was reasonable but was improved significantly by adjusting viscosity and compressibility parameters based on the observed

response, and it was shown that this updated model could predict the response to changes in electric field with good accuracy. This indicates that the model is in a form suitable for the developement of a control strategy. Further work should concentrate on developing a control strategy that functions well despite variations in the dampers response, due to environmental factors.

ACKNOWLEDGMENTS

One of the authors (NDS) is funded by an EPSRC research studentship.

REFERENCES

1. R. S. Sharp and S. A. Hassan 1986 *Proceedings IMechE* **D200**, 219–228. The relative performance capabilities of passive, active, and semi-active car suspension systems.
2. B. F. Spencer, R. E. Christenson and S. J. Dyke 1998 *Proceedings of the 2nd World Conference on Structural Control, Kyoto, Japan, 28 June–1 July*. Next generation benchmark control problem for seismically excited buildings.
3. B. F. Spencer, S. J. Dyke, M. K. Sain and J. D. Carlson 1996 *ASCE Journal of Engineering Mechanics* **123**, 230–238. Phenomenological model of a magnetorheological damper.
4. N. D. Sims, R. Stanway and A. R. Johnson 1999 *Shock and Vibration Digest* **31**, 195–203. Vibration control using smart fluids: a state-of-the-Art review.
5. Lord Corporation [mrfluid@lord.com] 1998 [http://www.webcom.com/mrfluid/damper.html]. Last updated 23/10/98.
6. R. Stanway, J. L. Sproston and N. G. Stevens 1987 *Journal of Electrostatics* **20**, 167–184. Non-linear modelling of an electro-rheological vibration damper.
7. D. R. Gamota and F. E. Filisko 1991 *Journal of Rheology* **35**, 399–426. Dynamic mechanical studies of electro-rheological fluids.
8. S. A. Burton, N. Makris, I. Konstatnopoulos and P. J. Antsaklis 1996 *ASCE Journal of Engineering Mechanics* **122**, 897–906. Modelling the response of an ER damper: phenomenology and emulation.
9. H. P. Gavin, R. D. Hanson and F. E. Filisko 1996 *ASME Journal of Applied Mechanics* **63**, 676–682. Electro-rheological dampers, Part II: testing and modelling.
10. D. J. Peel, R. Stanway and W. A. Bullough 1996 *Smart Materials and Structures* **5**, 591–606. Dynamic modelling of an ER vibration damper for vehicle suspension applications.
11. W. L. Wilkinson 1960 *Non-Newtonian Fluids*. Oxford: Pergamon Press.
12. D. J. Peel and W. A. Bullough 1994 *Proceedings IMechE* **C208**, 253–266. Prediction of ER valve performance in steady flow.
13. D. Karnopp 1985 *ASME Journal of Dynamic Systems* **107**, 100–103. Computer simulation of stick-slip friction in mechanical dynamic systems.
14. Simulink 1998 The Mathworks, Inc, Nattick, MA, U.S.A.
15. N. D. Sims, R. Stanway and S. Beck 1997 *Journal of Intelligent Material Systems and Structures* **8**, 426–433. Proportional feedback control of an electro-rheological vibration damper.

APPENDIX: NOTATION

$\bar{u}$	mean ER fluid velocity through ER valve
μ	fluid viscosity

χ	modified Bingham Plastic damper function
κ	bilinear spring function
π_1	friction coefficient
π_2	Reynolds number
π_3	Hedström number
ρ	fluid density
τ_b	ER fluid yield stress
ΔP	main piston differential pressure, i.e., pressure drop across the valve
A	effective main piston area
b	electrode gap breadth, i.e., circumference
E	electric field strength
F_y	yield force corresponding to ER fluid yield stress τ_b
h	electrode gap
k	lumped parameter stiffness term
l	ER valve length
m	lumped parameter mass term
Q	ER fluid flow rate through ER valve
u	piston velocity
x	model piston displacement
x_1	model damper displacement